Original Article
https://doi.org/10.5115/acb.19.101
pISSN 2093-3665 eISSN 2093-3673
Anatomy & Cell Biology acb

Position and size of the sphenoid door jamb in the lateral orbital wall for the orbital decompression

Kang-Jae Shin[1], Shin-Hyo Lee[2], Tae-Jun Ha[2], Hyun Jin Shin[3], Ki-Seok Koh[2], Wu-Chul Song[2], Doo-Jin Paik[4]
[1]Department of Anatomy and Cell Biology, Dong-A University College of Medicine, Busan, [2]Department of Anatomy, Research Institute of Medical Science, Konkuk University School of Medicine, Seoul, [3]Department of Ophthalmology, Konkuk University Medical Center, Konkuk University School of Medicine, Seoul, [4]Department of Medical Education, Hanyang University College of Medicine, Seoul, Korea

Abstract: The aim of this study was to identify the three-dimensional topography of the sphenoid door jamb (SDJ) in the lateral orbital wall and to propose navigational guidelines for safe deep lateral decompression using surgical landmarks. The 120 orbits and SDJs of 60 subjects were three-dimensionally reconstructed using Mimics software. The mean volumes of the orbit and SDJ were 24.3 mm^3 and 2.0 mm^3, respectively. The mean distances from the lateral orbital margin (LOM) to the anterior and posterior margins of the SDJ were 13.2 and 36.3 mm, respectively. The mean distances from the superior orbital fissure to the LOM and to the posterior margin of the SDJ were 40.2 mm and 4.6 mm, respectively. The mean distances from the inferior orbital fissure (IOF) to the anterior and posterior margins of the SDJ were 3.8 mm and 20.5 mm, respectively. In the superior approach of the orbit, it can be predicted that the area up to 3 cm posterior from the LOM is safe, while 1 cm posterior from the safe zone could be a dangerous zone. In the inferior approach of the orbit, the safe area will be about 1 cm posterior from the anterior tip of the IOF, and the area up to 1 cm posterior from the safe zone should be approached with extreme care.

Key words: Sphenoid doorjamb, Orbit, Orbital decompression, Graves disease

Received May 8, 2019; Accepted June 13, 2019

Introduction

Graves disease is an autoimmune disorder that is the most common cause of hyperthyroidism, and is more common in females than in males. The main clinical symptoms and sign are exophthalmos, motility disturbances of the extraocular muscles, and diplopia due to fibrosis and compression of the orbital contents. The enlargement of soft tissue by inflammatory edema within the bony orbit leads to not only abnormal exophthalmos but also optic neuropathy in severe cases [1-3].

Various orbital decompression techniques for Graves' disease have evolved since the condition was first described in 1911. There are now many clinical reports in the literature on surgical techniques, which are associated with variable amounts of proptosis reduction and complication rates [4-7]. Inferior, medial, and combined decompression (two- or three-wall decompression) approaches have been the most common procedures, but high frequencies of postoperative complications such as strabismus, diplopia, and globe displacement have been consistently reported [8-10]. Early lateral orbital decompression involved the removal of the anterior portion of the lateral orbital wall and did not achieve adequate volume expansion of the orbit [11].

Goldberg et al. [12] suggested deep lateral orbital decompression as a new surgical technique for removing the cortical

Corresponding author:
Doo-Jin Paik
Department of Medical Education, Hanyang Univesity College of Medicine, 222-1 Wangsimni-ro, Seongdong-gu, Seoul 04763, Korea
Tel: +82-2-2220-0603, Fax: +82-2-2281-7841, E-mail: paikdj@hanyang.ac.kr

bone of the greater wing of the sphenoid bone and the inner spongy bone between the superior orbital fissure (SOF) and the inferior orbital fissure (IOF). The obtained surgical space was designated as the sphenoid door jamb (SDJ) or the trigone because of it being shaped like a triangular prism [12, 13]. The SDJ is not an anatomical structure, but rather a potential space surrounded by three walls of the greater wing of the sphenoid bone. The anterior, posterior, and lateral walls of the SDJ are the orbital, cranial, and temporal surfaces of the greater wing of the sphenoid bone, respectively [14] (Fig. 1). Numerous previous studies have demonstrated the effectiveness of deep lateral orbital decompression in considerably reducing proptosis due to the SDJ being located just behind the globe, and with a very low frequency of postoperative complications such as the strabismus and diplopia [9, 15, 16]. While deep lateral orbital decompression has seemed the optimal surgical option, it has not yet become very popular among surgeons because of serious potential risks such as cerebrospinal fluid leakage and intracranial bleeding due to the large intersubject variations in SDJ topography [8, 12].

The present study performed three-dimensional (3D) investigations to identify the location, size, and shape of the SDJ in the lateral orbital wall, and to propose navigational guidelines for safe deep lateral decompression using surgical landmarks.

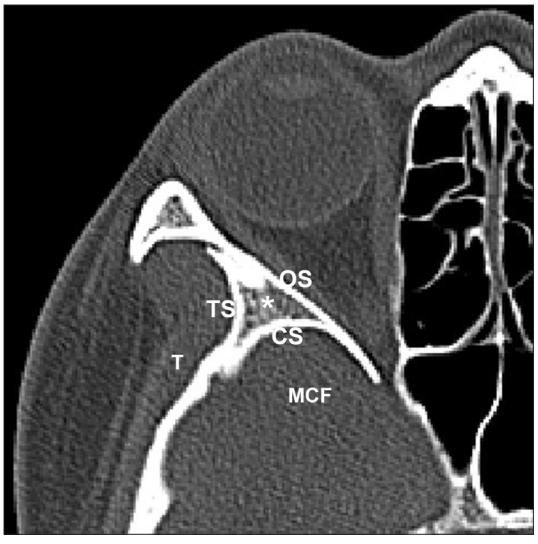

Fig. 1. Transverse plane of the sphenoid door jamb (SDJ). CS, the cranial surface of the SDJ; MCF, the middle cranial fossa; OS, the orbital surface of the SDJ; T, the temporalis muscle; TS, the temporal surface of the SDJ.

Materials and Methods

Subjects

Facial computed tomography (CT) scans were obtained of 60 patients (30 males and 30 females) who were hospitalized for medical reasons in the Department of Plastic and Reconstructive Surgery, Konkuk University Chungju Hospital. The absence of thyroid disease and any surgical history in the orbital region were confirmed in advance. The age range was 20–30 years, and the mean ages of the male and female patients were 24.1 and 24.0 years, respectively. All of the subjects were informed about the procedures and subsequently consented to participate prior to the commencement of the study. This study was approved by the Ethics Committee of Konkuk University Chungju Hospital for data collection (IRB No. KUCH 2014-042) and it was performed in accordance with the principles outlined in the Declaration of Helsinki.

CT scanning and 3D volume rendering

Serial facial CT images of the subjects were acquired under the following conditions: 120 kV, 75 mA, slice thickness of 1 mm, voxel size of 0.395 mm, and 512×512 pixels (Hispeed G, GE Healthcare, Niskayuna, NY, USA). The raw CT files were converted to clinical image files in DICOM format, and 3D volume rendering of the skull, orbit, and SDJ was performed using Mimics software (version 21, Materialise, Belgium). The SDJ and orbital space were then manually segmented in three dimensions because these regions would be identified as empty space if the software had been used (Fig. 2).

Measurements

Parameters such as the size and positional relationship of the SDJ were investigated at three levels based on consideration of the surgical approaches: the level of the SOF, level of the IOF, and the intermediate level of the SDJ. The volumes of the orbit and SDJ were calculated automatically using the computer software. The following measurements were made on the 120 3D reconstructed orbits of the 60 patients: (1) volume of the orbit, (2) volume of the SDJ; At the intermediate level of the SDJ: (3) distance from the lateral orbital margin (LOM) to the anterior margin of the SDJ, (4) distance from the LOM to the posterior margin of the SDJ, (5) width of the SDJ, (6) height of the SDJ, (7) distance from the orbital surface to the cranial surface of the SDJ, (8) distance from the orbital surface to the lateral surface of the SDJ; At the level of the SOF: (9) distance from the LOM to the SOF, (10) distance

https://doi.org/10.5115/acb.19.101

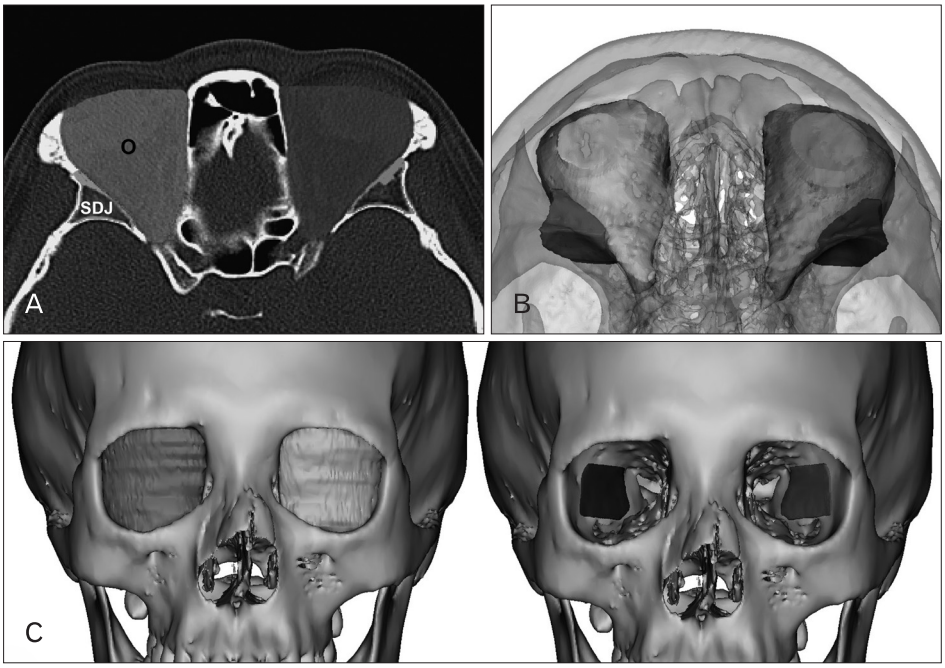

Fig. 2. Segmentation and 3D volume rendering of the orbit and sphenoid door jamb (SDJ). (A) the outlines of the orbit and SDJ by manual segmentation. (B) The superior view of reconstructed orbit and SDJ. (C) Frontal view reconstructed orbit and SDJ. O, orbit.

Table 1. Volume of the orbit and the SDJ

	Overall	Range
1. Volume of the orbit	24.3±2.7	18.5–31.5
2. Volume of the SDJ	2.0±0.6	1.0–3.7

Values are presented as mean±SD (mm^3). SDJ, sphenoid door jamb.

Table 2. The position and size of the SDJ at the intermediate level

	Overall	Range
3. Distance from the LOM to the anterior margin of the SDJ	13.2±1.9	7.0–18.0
4. Distance from the LOM to the posterior margin of the SDJ	36.3±2.8	28.7–43.3
5. Width of the SDJ	23.4±2.6	16.3–30.4
6. Height of the SDJ	19.1±2.1	14.5–24.9
7. Distance from the orbital surface to cranial surface of the SDJ	6.2±1.6	3.5–10.5
8. Distance from the orbital surface to lateral surface of the SDJ	7.1±1.5	3.9–12.2

Values are presented as mean±SD (mm). SDJ, sphenoid door jamb.

from the SOF to the posterior margin of the SDJ, (11) width of the SDJ; At the level of the IOF: (12) distance from the LOM to the IOF, (13) distance from the IOF to the anterior margin of the SDJ, (14) distance from the IOF to the posterior margin of the SDJ, (15) width of the SDJ.

Statistical analysis

Dependent-samples and independent-samples t-tests were performed using SPSS statistical software version 24 (IBM Corp., Armonk, NY, USA). The cutoff for statistical significance was set at $P<0.05$.

Results

None of the parameters analyzed in this study differed significantly with laterality or sex. The mean volumes of the orbit and the SDJ are listed in Table 1: they were 24.3 mm^3 (No. 1) and 2.0 mm^3 (No. 2), respectively. There was a large inter-subject variability in the volume of the SDJ (1.0–3.7 mm^3).

At the intermediate level of the SDJ (Table 2, Fig. 3), the mean distances from the LOM to the anterior and posterior margins of the SDJ were 13.2 mm (No. 3) and 36.3 mm (No. 4), respectively. The mean width and height of the SDJ were 23.4 mm (No. 5) and 19.1 mm (No. 6), respectively. The values of Nos. 7 and 8 indicated the depth limits of the SDJ that were removable for safe orbital expansion. The mean distances from the orbital surface to the cranial and temporal surfaces of the SDJ were 6.2 mm (No. 7) and 7.1 mm (No. 8), respectively.

At the levels of the SOF and IOF (Table 3, Fig. 4), the mean distances from the SOF to the LOM and to the posterior margin of the SDJ were 40.2 mm (No. 9) and 4.6 mm (No. 10), respectively. Measurement No. 10 reflecting the posterior limit of the SDJ that was removable almost corresponded to the anterior tip of the SOF (minimum, 1.3 mm) or was about 1 cm anterior from the anterior tip of the SOF (maximum, 10.4

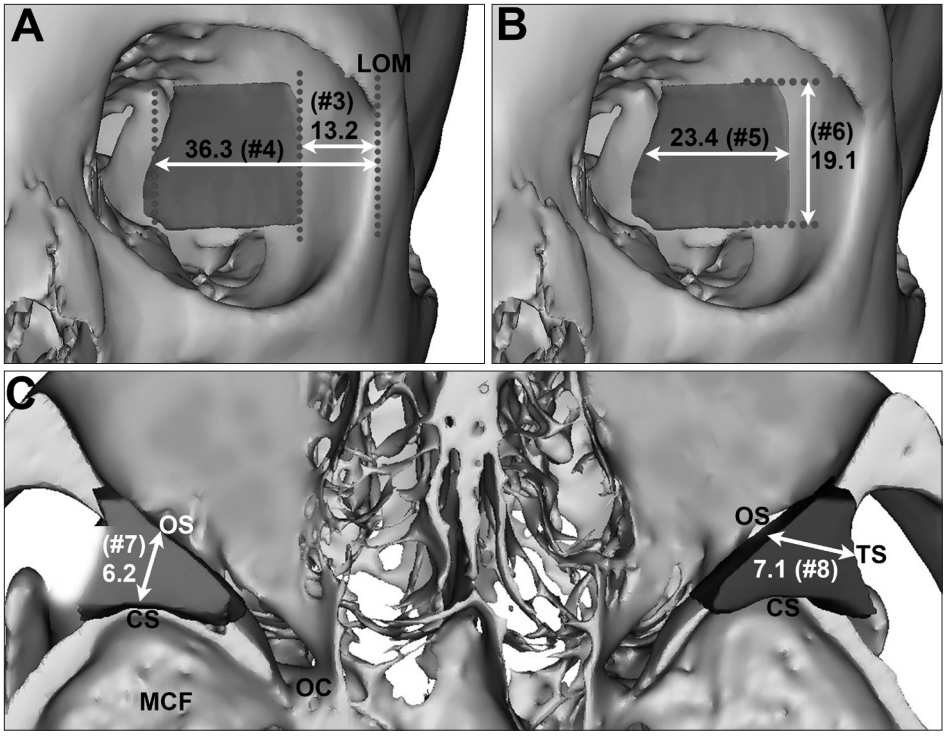

Fig. 3. (A–C) Mean distances of the sphenoid door jamb (SDJ) at the intermediated level (mm). CS, the cranial surface; LOM, the lateral orbital margin; MCF, the middle cranial fossa; OC, the optic canal; OS, the orbital surface; TS, the temporal surface.

Table 3. The position and size of the SDJ at the levels of the SOF and IOF

	Overall	Range
Level of the superior orbital fissure		
9. Distance from the LOM to the SOF	40.2±3.8	31.8–49.8
10. Distance from the SOF to the posterior margin of the SDJ	4.6±2.0	1.3–10.4
11. Width of the SDJ	18.2±3.9	9.8–42.5
Level of the inferior orbital fissure		
12. Distance from the LOM to the IOF	16.4±1.8	12.6–20.7
13. Distance from the IOF to the anterior margin of SDJ	3.8±1.6	0.7–9.0
14. Distance from the IOF to the posterior margin of the SDJ	20.5±3.3	10.4–29.0
15. Width of the SDJ	24.3±3.2	13.1–32.6

Values are presented as mean±SD (mm). SDJ, sphenoid door jamb; SOF, superior orbital fissure; IOF, inferior orbital fissure; LOM, lateral orbital margin.

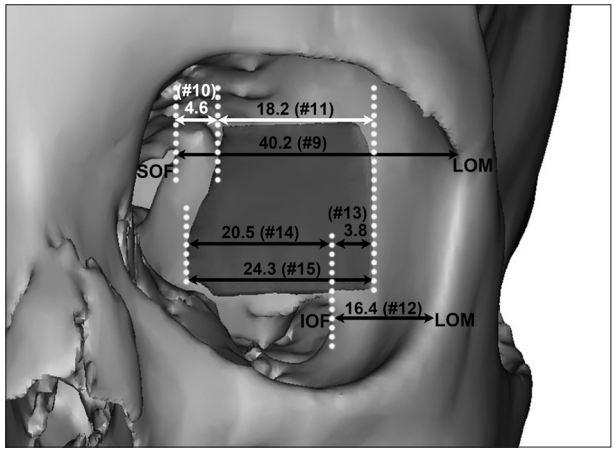

Fig. 4. Mean distances of the sphenoid door jamb at the superior orbital fissure (SOF) and inferior orbital fissure (IOF) level (mm). LOM, lateral orbital margin.

mm). The mean distance from the LOM to the IOF was 16.4 mm (No. 12), and the mean distances from the IOF to the anterior and posterior margins of the SDJ were 3.8 mm (No. 13) and 20.5 mm (No. 14), respectively. The values of Nos. 13 and 14—which correspond to the positions of the anterior and posterior limits of the SDJ that were removable—varied markedly between the individuals (No. 13, 0.7–9.0 mm; No. 14, 10.4–29.0 mm).

Some additional values calculated by subtracting or summing the values presented in Tables 2 and 3 are listed in Table 4;

Table 4. Position of anterior and posterior limits and width of the SDJ according to three levels

	LOM–anterior margin of the SDJ	LOM–posterior margin of the SDJ	Width
SOF level	17.4	35.6	18.2
Intermediate level	13.2	36.3	23.4
IOF level	12.6	36.9	24.3

Values are presented as mean (mm). SDJ, sphenoid door jamb; LOM, lateral orbital margin; SOF, superior orbital fissure; IOF, inferior orbital fissure.

https://doi.org/10.5115/acb.19.101

for example, No. 9 minus No. 10 minus No. 11 corresponds to the distance from the LOM to the anterior margin of the SDJ at the level of the SOF, and No. 12 minus No. 13 corresponds to the distance from the LOM to the anterior margin of the SDJ at the level of the IOF. The mean distances from the LOM to the anterior and posterior margins of the SDJ differed according to the level. The width of the SDJ also varied with the level, being somewhat larger at the level of the IOF (24.3 mm) than at the level of the SOF (18.2 mm).

Discussion

Deep lateral orbital decompression based on the detailed anatomy of the SDJ was first reported in 1998. The area removable in deep lateral orbital decompression has been classified into three portions: the lacrimal keyhole, the SDJ, and the basin of the IOF [12]. The lacrimal keyhole is a wedge-shaped area from the fossa of the lacrimal gland anteriorly, and to the lesser wing of the sphenoid bone posteriorly. It is limited laterally by the temporalis muscle, and medially by the point where the orbital roof thins to the orbital plate of the frontal bone. The lacrimal keyhole can provide substantial space into which the orbital adipose tissue can prolapse superolaterally. The basin of the IOF consists of the zygomatic bone and the lateral portion of the maxilla. Removing zygomatic bone until a thin bony rim remains along the LOM and the lateral portion of the maxillary sinus roof will allow the inferolateral prolapse of orbital adipose tissue. The SDJ is the main target of deep lateral decompression because it has the largest volume among the three portions, and the effectiveness of the proptosis reduction is greatest due to its positional relationship to the globe.

An accurate understanding of the SDJ boundaries is essential for ensuring that surgeons can perform safe procedure. The posterior boundary of the SDJ (the cranial surface of the greater wing of the sphenoid bone) is a very thin cortical bone that forms the anterior boundary of the middle cranial fossa, and it is recommended to preserve this in order to prevent cerebrospinal fluid leakage. The medial and lateral corners of the posterior wall are located deeper because of the anterior curvature of the posterior wall. This structural feature impairs the surgical view, and so surgeons need to change their standing position from the ipsilateral side of the operated orbit to the contralateral side or the opposite direction in order to maximize bone removal [17]. The superior boundary of the SDJ is also cortical bone, and it corresponds to a sharp bony crest of the lesser wing of the sphenoid bone separating the anterior and middle cranial fossae. The orbital roof and the SOF could become crucial surgical landmarks because the superior boundary of the SDJ is parallel to the orbital roof, and the medial extension continues to the SOF. The superior and posterior boundaries of the SDJ smoothly merge adjacent to the SOF. The superior boundary should be gradually ground down from the anterior portion of the orbital roof [18]. Despite numerous explanations of the SDJ, many ophthalmic surgeons may still hesitate to choose deep lateral orbital decompression because there is little scientific evidence that it prevents serious surgical complications, which is probably due to the large intersubject variability.

The measured SDJ volume has differed somewhat among studies using CT. Values both larger (2.9 cm^3 [12] and 2.84 cm^3 [19]) and smaller (1.24 cm^3 [13] and 0.428 cm^3 [20]) than that found in the present study (2.0 cm^3) have been reported. These discrepancies may have been due to methodological differences such as in the slice thickness and different decisions about the SDJ outline. The volume of the SDJ is calculated by multiplying the area of the outlined structure by the thickness of each scan slice. Goldberg et al. [12] scanned nine patients and 11 normal subjects with slice thicknesses of 1.5–3.0 mm, Beden et al. [13] and Oh and Lee [19] used 0.5-mm-thick CT sections of 20 normal patients, and Kim et al. [20] scanned 20 patients using a slice thickness of 2.5 mm. These differences in scan thickness among the different studies may have greatly influenced the calculated volumes of the SDJ.

In addition, determining the inferior boundary of the SDJ on CT images is a complicated process that depends on the skill of the investigators. Goldberg et al. [12] described the SDJ as being located in the greater wing of the sphenoid bone between the SOF and IOF, which means that its inferior boundary is the IOF. However, when grinding the SDJ of the cadavers in the present study it was often found that the SDJ could be ground slightly deeper at its inferior portion than at the level of the IOF. This indicates that there is a difference between what can be obtained in practice and what is found when utilizing CT. The authors of the present study thought that the actual space available is wider, and the precise description of the inferior boundary of the SDJ should be changed to the infratemporal surface of the greater wing of the sphenoid bone. Also, the variations of the SDJ volume in the literature may be reflecting different decisions about the location of the inferior boundary of the SDJ in CT images.

The amount of proptosis reduction after only deep lateral

orbital decompression in the SDJ was previously reported to range from 0.8 to 2.7 mm per 1 cm^3 [12, 20]. This wide variation may be attributable to differences in the surgical techniques and experience levels of the surgeons. For example, it is recommended to preserve the posterior and lateral boundaries of the SDJ in order to prevent complications, but intentional dural exposure at the posterior boundary and leaving only a thin shell at the lateral boundary are helpful for confirming the depth of the SDJ and will maximize bone removal [12, 17]. Based on the results of our study, the mean proptosis reduction could be estimated to range from 1.6 mm (0.8 mm × 2.0 cm^3) to 5.4 mm (2.7 mm × 2.0 cm^3), and theoretically it can also be predicted that the amount of exophthalmos reduction ranges up to a maximum of about 1 cm (2.7 mm × 3.7 cm^3).

In the present study, the distance from the LOM to the anterior margin of the SDJ at the level of the SOF was 17.4 mm, which is very close to the value of 18.2 mm obtained for dried skulls from the same racial group [19]. That previous study used the frontosphenoidal suture as a landmark for the anterior margin of the SDJ. Although that value was similar to the one obtained in our study, using a bony landmark such as a suture is not practical because the suture could be indistinguishable in the procedure and vary between individuals. A value of 20.5 mm was obtained for dried skulls of Turkish subjects [13]. This difference from our study may be caused by differences between the investigated racial groups and between the methods used to identify the SDJ outline. That previous study identified the location of the SDJ by shining light on the dried skull from the lateral side, which might only vaguely reveal the outline of the SDJ.

The distance from the LOM to the anterior margin of the SDJ differed according to the level, being 17.4 mm at the level of the SOF, 13.2 mm at the intermediate level of the SDJ, and 12.6 mm at the level of the IOF. This variation could be attributed to the geometry of the orbit, since the orbital margins are curved posteriorly and the superior margin protrudes more than the inferior margin [21]. Therefore, the distance from the LOM to the anterior margin of the SDJ increased at a higher level.

In contrast, the distance from the LOM to the posterior margin of the SDJ showed the opposite trend, decreased slightly at higher levels: 35.6 mm at the level of the SOF, 36.3 mm at the intermediate level of the SDJ, and 36.9 mm at the level of the IOF. Given that the superior margin of the orbit is generally positioned more anteriorly, these results indicate that the position of the anterior margin of the SDJ is relatively constant regardless of the level, while the posterior margin is located more posteriorly at a lower level. The width of the SDJ demonstrated the morphological difference between the anterior and posterior margins of the SDJ, being 18.2 mm at the level of the SOF, 23.4 mm at the intermediate level of the SDJ, and 24.3 mm at the level of the IOF. The location of the posterior margin of the SDJ has been previously reported to vary between 26.0 and 36.9 mm [19, 22, 23]. The present study identified the SDJ as a triangular prism with a height of about 2 cm and whose bottom is wider than its top. The findings for the positions of the anterior and posterior margins and overall shape of the SDJ represent crucial information for ensuring safe and maximum decompression.

The deep lateral orbital wall can be approached from the superior or inferior direction of the orbit via lateral canthal, lateral eyelid crease, or lateral transconjunctival incisions [12, 24], for which the SOF and IOF may be useful surgical landmarks. In the superior approach using the SOF as the surgical landmark, surgeons should keep in mind the positional relationship of the anterior and posterior margins of the SDJ and the distance from the SOF to the removable posterior limit of the SDJ. The navigational guidelines for the safe deep lateral orbital decompression was presented in Fig. 5. The mean distance from the LOM to the SOF was about 4 cm. The mean distance from the LOM to the anterior margin of the SDJ was 17.4 mm, which was about half the mean distance from the LOM to the posterior margin (35.6 mm). In other words, the

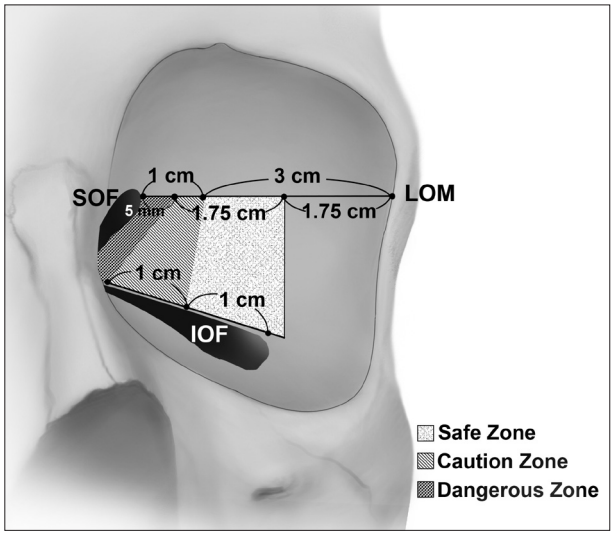

Fig. 5. The navigational guidelines for the effective and safe deep lateral orbital decompression. IOF, inferior orbital fissure; LOM, lateral orbital margin; SOF, superior orbital fissure.

https://doi.org/10.5115/acb.19.101

ratio between the distance from the LOM to the anterior margin of the SDJ and the distance from the anterior to posterior margins of the SDJ can be considered to be 1:1. The mean distance from the SOF to the removable posterior limit of the SDJ was about 5 mm. This is a dangerous area because the anterior and posterior walls of the SDJ converge to a single wall. Surgeons who prefer the superior approach of the orbit need to be fully aware of the large intersubject variability in the size of the dangerous zone (1.3–10.4 mm). The maximum value of 10.4 mm indicates that the anterior and posterior walls of the SDJ could be encountered quite early according to the patient, and that the dangerous zone extends up to 1 cm from the SOF. From these observations it can be predicted that 3 cm posterior from the LOM is safe, and although 1 cm posterior could be the dangerous zone, the rest of the spongy bone filling the SDJ designated as the 'caution zone' should be removed up to about 5 mm posterior from the safe zone via delicate handling of the drill in order to achieve the maximum orbital expansion. Some authors have suggested that the removal of the deep lateral wall should commence inferiorly from adjacent to the IOF and extend superolaterally [8, 13]. The mean distance from the anterior tip of the IOF to the posterior margin of the SDJ was about 2 cm, but the safe area will be about 1 cm posterior from the anterior tip of the IOF based on consideration of the minimum value of 10.4 mm. The caution zone up to 1 cm posterior from the safe zone should be approached with extreme care.

The present study has identified the position, size and shape of the SDJ in the deep lateral orbital wall via 3D volume rendering, and has also yielded new navigational guidelines that will facilitate effective and safe deep lateral orbital decompression.

ORCID

Kang-Jae Shin: https://orcid.org/0000-0001-8703-9220
Shin-Hyo Lee: https://orcid.org/0000-0001-7031-7722
Tae-Jun Ha: https://orcid.org/0000-0003-1192-8456
Hyun Jin Shin: https://orcid.org/0000-0002-3563-8042
Ki-Seok Koh: https://orcid.org/0000-0003-2861-4031
Wu-Chul Song: https://orcid.org/0000-0001-9678-1830
Doo-Jin Paik: https://orcid.org/0000-0001-9617-9452

Author Contributions

Conceptualization: WCS, DJP. Data acquisition: KJS, SHL, TJH. Data analysis or interpretation: KJS, TJH, WCS, DJP. Drafting of the manuscript: KJS, SHL. Critical revision of the manuscript: HJS, KSK. Approval of the final version of the manuscript: all authors.

Conflicts of Interest

No potential conflict of interest relevant to this article was reported.

Acknowledgements

This work was supported by the research fund of Hanyang University (HY-2018-2457).

References

1. Bahn RS. Graves' ophthalmopathy. N Engl J Med 2010;362:726-38.
2. Choi SW, Lee JY, Lew H. Customized orbital decompression surgery combined with eyelid surgery or strabismus surgery in mild to moderate thyroid-associated ophthalmopathy. Korean J Ophthalmol 2016;30:1-9.
3. Khoo TK, Bahn RS. Pathogenesis of Graves' ophthalmopathy: the role of autoantibodies. Thyroid 2007;17:1013-8.
4. Leong SC, White PS. Outcomes following surgical decompression for dysthyroid orbitopathy (Graves' disease). Curr Opin Otolaryngol Head Neck Surg 2010;18:37-43.
5. Baldeschi L. Small versus coronal incision orbital decompression in Graves' orbitopathy. Orbit 2010;29:177-82.
6. Cascone P, Rinna C, Reale G, Calvani F, Iannetti G. Compression and stretching in Graves orbitopathy: emergency orbital decompression techniques. J Craniofac Surg 2012;23:1430-3.
7. Verity DH, Rose GE. Acute thyroid eye disease (TED): principles of medical and surgical management. Eye (Lond) 2013;27:308-19.
8. Baldeschi L, MacAndie K, Hintschich C, Wakelkamp IM, Prummel MF, Wiersinga WM. The removal of the deep lateral wall in orbital decompression: its contribution to exophthalmos reduction and influence on consecutive diplopia. Am J Ophthalmol 2005;140:642-7.
9. Goldberg RA. Old wine and new wine. Arch Ophthalmol 2000;118:1006-7.
10. Abràmoff MD, Kalmann R, de Graaf ME, Stilma JS, Mourits MP. Rectus extraocular muscle paths and decompression surgery for Graves orbitopathy: mechanism of motility disturbances. Invest Ophthalmol Vis Sci 2002;43:300-7.
11. McCord CD Jr. Current trends in orbital decompression. Ophthalmology 1985;92:21-33.
12. Goldberg RA, Kim AJ, Kerivan KM. The lacrimal keyhole, orbital door jamb, and basin of the inferior orbital fissure: three ar-

eas of deep bone in the lateral orbit. Arch Ophthalmol 1998;116: 1618-24.
13. Beden U, Edizer M, Elmali M, Icten N, Gungor I, Sullu Y, Erkan D. Surgical anatomy of the deep lateral orbital wall. Eur J Ophthalmol 2007;17:281-6.
14. Feneis H, Dauber W. Anatomisches Bildwörterbuch der internationalen Nomenklatur. Stuttgart: Thieme; 1998.
15. Unal M, Ileri F, Konuk O, Hasanreisogğlu B. Balanced orbital decompression in Graves' orbitopathy: Upper eyelid crease incision for extended lateral wall decompression. Orbit 2000;19:109-17.
16. Mehta P, Durrani OM. Outcome of deep lateral wall rim-sparing orbital decompression in thyroid-associated orbitopathy: a new technique and results of a case series. Orbit 2011;30:265-8.
17. Kakizaki H. Advantageous surgeon's position in deep lateral orbital wall decompression. Orbit 2011;30:131.
18. Takahashi Y, Miyazaki H, Ichinose A, Nakano T, Asamoto K, Kakizaki H. Anatomy of deep lateral and medial orbital walls: implications in orbital decompression surgery. Orbit 2013;32: 409-12.
19. Oh DH, Lee JK. Surgical anatomy of deep lateral wall by adults cadavers and computed tomography. J Korean Ophthalmol Soc 2011;52:964-9.
20. Kim KW, Byun JS, Lee JK. Surgical effects of various orbital decompression methods in thyroid-associated orbitopathy: computed tomography-based comparative analysis. J Craniomaxillofac Surg 2014;42:1286-91.
21. Kamer L, Noser H, Kirsch E, Hammer B. Anatomy-based surgical concepts for individualized orbital decompression surgery in graves orbitopathy. II. Orbital rim position and angulation. Ophthalmic Plast Reconstr Surg 2012;28:251-5.
22. Kakizaki H, Nakano T, Asamoto K, Iwaki M. Posterior border of the deep lateral orbital wall: appearance, width, and distance from the orbital rim. Ophthalmic Plast Reconstr Surg 2008;24: 262-5.
23. Lee H, Lee Y, Ha S, Park M, Baek S. Measurement of width and distance of the posterior border of the deep lateral orbital wall using computed tomography. J Craniomaxillofac Surg 2011;39: 606-9.
24. Rootman DB. Orbital decompression for thyroid eye disease. Surv Ophthalmol 2018;63:86-104.